UNIVERSITY
OF TRENTO

DIPARTIMENTO DI INGEGNERIA E SCIENZA DELL'INFORMAZIONE

38123 Povo – Trento (Italy), Via Sommarive 14
http://www.disi.unitn.it

SYNTHESIS OF TIME-MODULATED PLANAR ARRAYS WITH
CONTROLLED HARMONIC RADIATIONS

P. Rocca, L. Poli, G. Oliveri, and A. Massa

January 2011

Technical Report # DISI-11-099

Synthesis of Time-Modulated Planar Arrays with Controlled Harmonic Radiations

P. Rocca, L. Poli, G. Oliveri, and A. Massa

ELEDIA Research Group

Department of Information Engineering and Computer Science

University of Trento, Via Sommarive 14, 38050 Trento - Italy

Tel. +39 0461 882057, Fax +39 0461 882093

E-mail: {*paolo.rocca, lorenzo.poli, giacomo.oliveri*}*@disi.unitn.it*

1

Synthesis of Time-Modulated Planar Arrays with Controlled Harmonic Radiations

P. Rocca, L. Poli, G. Oliveri, and A. Massa

Abstract

This paper presents a technique for the control of the sideband radiations in time-modulated planar arrays. The proposed method is aimed at generating a desired pattern at the carrier frequency as well as reducing the power losses and the interferences related to the harmonic radiations. By acting on both the durations and the commutation instants of the time pulses controlling the element switches, the method based on a Particle Swarm Optimizer is applied. Representative results are reported and discussed to show the effectiveness of the proposed approach.

Key words: Time Modulation, Planar Arrays, Pattern Synthesis, Particle Swarm Optimization.

1 Introduction

The use of time as an additional degree of freedom to increase the flexibility of the antenna design has been introduced in [1]. Such a strategy was first exploited by Kummer *et al.* [2] to obtain average ultra-low sidelobes patterns by controlling the aperture excitations. The excitations were modulated through an on-off sequence enforced by a set of radio-frequency (RF) switches in the beam forming network. The reconfigurability of the radiated pattern starting from an initial pattern afforded by static excitations having reduced dynamic range [3][4] or from a uniform distribution [5]-[7] has been widely investigated, as well.

The main drawback of the time control is the presence of unwanted harmonic radiations, the so-called sideband radiation (SBR), generated by the periodic commutation between the on and off states of the RF switches. Suitable optimization approaches based on stochastic evolutionary algorithms (e.g., differential evolution [8] or simulated annealing [5]) have been used to reduce the power losses by minimizing the sideband level (SBL), namely the peak level of the sideband radiation with respect to the maximum radiation intensity achieved at the central frequency. However, when dealing with time-modulated planar arrays ($TMPA$), suitable to control and shape the radiation diagram in three dimensions as needed in several applications [11][12], the SBR reduction through the minimization of the SBL turns out to be more critical and cumbersome than in linear arrays because of the iterative computation of the SBL during the optimization process requires the generation of the harmonic patterns [3][4][9][10]. To overcome this drawback, a closed-form expression quantifying in a direct way the total amount of power losses (i.e., the SBR) has been derived in [13] for linear arrays and properly exploited in [14] for an efficient antenna design. On the other hand, it has been recently proved [20] that additional parameters for the control of the pulse sequence can be suitably introduced to decrease the SBL modifying neither the pattern radiated at the carrier frequency nor the SBR. In this paper, the control of the SBR in $TMPA$ is dealt with an analytic expression (i.e., the extension of that derived in [13] for one-dimensional geometries) to count the power losses in $TMPA$. Besides the optimization of the time-duration of the modulation sequence and likewise the approach in [20], the optimization of the *on-off commutation instants* is also performed by means of the Particle Swarm Optimizer (PSO) [16]. The synthesis of Taylor-like sum patterns

with low sidelobes using $TMPA$s with square lattices and circular boundaries is addressed. The outline of this paper is as follows. The $TMPA$ synthesis and the optimization problem at hand are mathematically formulated in Section 2. A set of representative results is reported and discussed (Section 3) to provide an evidence of the effectiveness of the proposed method. Eventually, some conclusions are drawn (Section 4).

2 Mathematical Formulation

The field radiated by a $TMPA$ of isotropic sources lying on the xy plane is

$$E\left(u,v,t\right) = e^{j\omega_0 t}\sum_{m=0}^{M-1}\sum_{n=0}^{N-1}I_{mn}U_{mn}\left(t\right)e^{j(mu+nv)} \tag{1}$$

where ω_0 is the angular frequency of the carrier signal and $\underline{I} = \{I_{mn},\ m = 0,...,M-1,\ n = 0,...,N-1\}$ is the set of static (complex) array excitations. Moreover, $u = kd_x\sin\theta\cos\phi$ and $v = kd_y\sin\theta\sin\phi$, $k = \frac{\omega_0}{c}$ is the wavenumber of the background medium, c being the speed of light in vacuum, and d_x, d_y are the inter-element spacings along the Cartesian axes. The periodic function $U_{mn}\left(t\right)$ models the time-modulation obtained through the RF switches. It is a pulse function of unitary amplitude, period T_p, and duration $\Delta t_{mn} = t_{mn}^{off} - t_{mn}^{on}$, t_{mn}^{on} and t_{mn}^{off} being the on-off commutation instants, respectively, such that $U_{mn}\left(t\right) = 1$ when $t_{mn}^{on}\leq t\leq t_{mn}^{off}$ while $U_{mn}\left(t\right) = 0$ otherwise.

By substituting the Fourier expansion of $U_{mn}\left(t\right)$ in (1), the radiated field can be expressed as a sum of an infinite number of harmonic components, $E\left(u,v,t\right) = \sum_{h\in\mathbb{Z}}E_h\left(u,v,t\right)$, whose h-th term is

$$E_h\left(u,v,t\right) = e^{j(\omega_0+h\omega_p)t}\sum_{m=0}^{M-1}\sum_{n=0}^{N-1}I_{mn}u_{mnh}e^{j(mu+nv)} \tag{2}$$

where $\omega_p = \frac{2\pi}{T_p}$ and $u_{mnh} = \frac{1}{T_p}\int_{-\frac{T_p}{2}}^{\frac{T_p}{2}}U_{mn}\left(t\right)e^{-jh\omega_p t}dt$. When $h = 0$, the Fourier coefficients are equal to $u_{mn0} = \frac{\Delta t_{mn}}{T_p} = \tau_{mn}$ and $E_0\left(u,v,t\right) = e^{j\omega_0 t}\sum_{m=0}^{M-1}\sum_{n=0}^{N-1}I_{mn}\tau_{mn}e^{j(mu+nv)}$, τ_{mn} being the normalized pulse duration of the mn-th element. Otherwise ($h\neq 0$), the coefficients turn out to be

$$u_{mnh} = \frac{e^{-jh\omega_p t_{mn}^{on}} - e^{-jh\omega_p(\tau_{mn}T_p+t_{mn}^{on})}}{j2\pi h}. \tag{3}$$

Starting from the conclusions drawn in [13] and following the same line of reasoning, the power

radiated by a $TMPA$ in the harmonic radiations amounts to

$$\mathcal{P}_{SBR} = \frac{1}{T_p} \int_{-T_p/2}^{T_p/2} \left[\int_0^{2\pi} \int_0^\pi Re\left\{E_h\left(\theta, \phi, t\right)\right\}^2 \sin\theta d\theta d\phi \right] dt \tag{4}$$

which can be rewritten as

$$\mathcal{P}_{SBR} = \frac{1}{2} \sum_{h=-\infty, h\neq 0}^{\infty} \int_0^{2\pi} \int_0^\pi \left|\epsilon_{mn}\left(\theta, \phi\right)\right|^2 \sin\theta d\theta d\phi. \tag{5}$$

where $\epsilon_{mn}\left(\theta, \phi\right) = \sum_{m=0}^{M-1} \sum_{n=0}^{N-1} I_{mn} u_{mnh} e^{jk\sin\theta(md_x\cos\phi + nd_y\sin\phi)}$. Since $\left|\epsilon_{mn}\left(\theta, \phi\right)\right|^2 = \left[\epsilon_{mn}\left(\theta, \phi\right)\right]\left[\epsilon_{rs}\left(\theta, \phi\right)\right.$

and

$$\sum_{h=-\infty, h\neq 0}^{\infty} u_{mnh} u_{rsh} = \hat{\tau} - \tau_{mn}\tau_{rs} \tag{6}$$

$m, r \in [0, ..., M-1]$, $n, s \in [0, ..., N-1]$, where $\hat{\tau} = \tau_{mn}$ if $\tau_{mn} \leq \tau_{rs}$ and $\hat{\tau} = \tau_{rs}$ otherwise [13], (5) reduces to the closed-form relationship given by

$$\begin{aligned} \mathcal{P}_{SBR} = 2\pi \sum_{m=0}^{M-1} \sum_{n=0}^{N-1} \sum_{r=0}^{M-1} \sum_{s=0}^{N-1} \left[Re\left\{I_{mn}I_{rs}^*\right\}\right. \\ sinc\left(k\sqrt{\left[(m-r)d_x\right]^2 + \left[(n-s)d_y\right]^2}\right)\left(\hat{\tau} - \tau_{mn}\tau_{rs}\right)\right] \end{aligned}. \tag{7}$$

It is worth noticing that, once the geometry of the planar array is given (i.e., d_x and d_y are fixed), $\mathcal{P}_{SBR}$ is just a function of the static excitations $\underline{I}$ and of the normalized pulse durations $\underline{\tau} = \{\tau_{mn}, m = 0, ..., M-1, n = 0, ..., N-1\}$ to be optimized for synthesizing a desired pattern at the carrier frequency and jointly reducing the power wasted in the SBR.

Supposing a symmetric distribution of the excitation weights, the synthesis of $TMPA$s aimed at affording a sum pattern with a desired main beam, low sidelobes and reduced SBR can then be obtained through the minimization of the following cost function

$$\begin{aligned} \Psi_{SBR}\left\{\underline{I}, \underline{\tau}\right\} = & w_{BW}\left.\frac{\left|E_0^{ref}\left(u, v\right) - E_0\left(u, v; \underline{I}, \underline{\tau}\right)\right|^2}{\left|E_0^{ref}\left(u, v\right)\right|^2}\right|_{(u,v)\in\Theta_{BW}} + \\ & w_{SLL}\frac{\left|SLL^{ref} - SLL\left(\underline{I}, \underline{\tau}\right)\right|^2}{\left|SLL^{ref}\right|^2} + w_{SBR}\frac{\mathcal{P}_{SBR}\left(\underline{I}, \underline{\tau}\right)}{\mathcal{P}_{TOT}\left(\underline{I}, \underline{\tau}\right)} \end{aligned} \tag{8}$$

where $E_0^{ref}\left(u, v\right)$ and $E_0\left(u, v; \underline{I}, \underline{\tau}\right)$ are the reference radiation pattern and the current one at ω_0, Θ_{BW} being the main lobe region. Moreover, SLL^{ref} and $SLL\left(\underline{I}, \underline{\tau}\right) = max_{(u,v)\in\Theta_{SLL}}\left\{E_0\left(u, v; \underline{I}, \underline{\tau}\right)\right\}$ are the reference and the current peak levels of the secondary lobes at ω_0, Θ_{SLL} being the side-

lobe region. Finally, $\mathcal{P}_{TOT}(\underline{I}, \underline{\tau})$ is the total power radiated by the $TMPA$ and w_{BW}, w_{SLL} and w_{SBR} are real and positive weight coefficients aimed at privileging the optimization of some terms of 8.

As far as the control of the harmonic radiations is concerned, the on-off commutation instants $\underline{t}^{on}$ can be also and taken into account to shape the patterns at $h \neq 0$. As a matter of fact, the modifications of the values t_{mn}^{on}, $\forall mn$, have a direct impact on the Fourier coefficients of the harmonic radiations (3), while they affect neither the SLL (keeping unaltered the pattern at the carrier frequency) nor the $\mathcal{P}_{SBR}$. Therefore, the peak level of the sideband radiations can be reduced by acting on $\underline{t}^{on}$ to minimize the following cost function

$$\Psi_{SBL}\{\underline{t}^{on}\} = \sum_{h=1}^{H} SBL_h\left(\underline{t}^{on}\right) \tag{9}$$

where SBL_h is the sideband level in correspondence with the h-th harmonic radiation. The goal is to exploit these additional degrees of freedom $\underline{t}^{on}$ to spread as uniformly as possible the power over the whole angular range (i.e., $\theta \in [0^o, 90^o]$, $\phi \in [0^o, 360^o]$).

The optimization of (8) and of (9) is carried out sequentially through a PSO-based [16] strategy. More specifically, the inertial weight version of the PSO used in [17][18] is considered hereinafter. A $2D$-FFT subroutine is used for the generation of the beam patterns to improve the efficiency of the method.

3 Numerical Results

In this section, a set of representative results are reported to give some indications on the performances of the proposed strategy. The benchmark geometry is a planar array with circular contour $r = 5\lambda$ in radius, whose radiating elements are placed on a square lattice of $N \times M = 20 \times 20$ elements equally-spaced by $d_x = d_y = 0.5\lambda$. The number of active elements turns out being equal to $\Lambda = 316$. The static array configuration, shown in Fig. 1 together with the corresponding quiescent pattern, has been set to that of a Taylor sum pattern (i.e., $\underline{I} = \underline{I}^T$) with $SLL = -30\,dB$ and $\bar{n} = 6$ [19]. Since the Taylor excitations have a quadrantal symmetry, only $\Lambda/4$ elements have been optimized.

At the first stage, the minimization of the cost function (8) has been performed by optimizing

the pulse durations, $\underline{\tau}$. As far as the PSO is concerned, a swarm of $P = 30$ particles has been used, while the inertial weight (ω), the cognitive (C_1) and social (C_2) acceleration coefficients have been set to $w = 0.4$ and $C_1 = C_2 = 2$, respectively, according to the guidelines of [20]. Moreover, $SLL^{ref} = -40\,dB$, $w_{BW} = w_{SLL} = 2$, and $w_{SBR} = 1$.

After $K = 2000$ iterations and a CPU time of the same order in magnitude of [9] thanks to the use of a 2D FFT combined with a PSO to speed up the synthesis process, the pulse sequence $\underline{\tau}^{opt}$ in Fig. 2(a) and the corresponding pattern at the carrier frequency in Fig. 2(b) have been determined. The peak sidelobe level of the synthesized pattern is equal to $SLL^{opt} = -37.8\,dB$, that is $7.8\,dB$ lower than that of the quiescent distribution. The power losses amount to $\mathcal{P}_{SBR}\left(\underline{I}^T, \underline{\tau}^{opt}\right) = 13.2\%$ of the total radiated power and the directivity in the boresight direction, computed as in [9], is $D^{max} = 24.4\,dB$. As regards the power distribution, the patterns at $h = 1$ and $h = 2$ are shown in Fig. 3(a) and Fig. 3(b), respectively. The peak level of the sideband radiation is obtained in correspondence with the first harmonic term and it is equal to $SBL_1 = -16.15\,dB$ while $SBL_2 = -21.88\,dB$. Moreover, it also results that a significant portion of the power radiated in the SBR lies within the main lobe region.

The non-uniform distribution of the wasted power can be efficiently addressed by minimizing at the second stage the functional in (9). For simplicity, only the first harmonic term has been optimized (i.e., $H = 1$) to keep a reasonable trade-off between computational efficiency and SBL reduction. Such a choice is justified since the power contribution reduces as $|h|$ increases [13] and the optimization of the first harmonics is usually enough. The pulse sequence is shown in Fig. 4 where the index t indicates the array element according to the following rule: $t = n + 1 + m \times M$, $m, n = 0, ..., N - 1$. The plots of the optimized power patterns in correspondence with the first two harmonic terms are given in Fig. 5. The SBL at $h = 1$ turns out to be reduced from $-16.15 dB$ down to $-33.66\,dB$ with a non-negligible improvement of about $17.5\,dB$. On the other hand, it is worth noticing that also the value of SBL_2 has been improved by more than $11\,dB$ from $-21.88\,dB$ [Fig. 3(b)] down to $-32.10\,dB$ [Fig. 5(b)]. For the sake of completeness, the value of SBL_h in correspondence with the first 20 harmonic modes has been computed (Fig. 6), as well. As it can be observed, its values are below those of the solution at the first stage (i.e., when $t_{mn}^{on} = 0$, $\forall mn$) when optimizing $\underline{t}^{on}$, even though only

7

SBL_1 ($h = H = 1$) has been taken into account at the second stage of the synthesis process. Quantitatively, the improvement turns out to be $-12.15 \, dB$ on average with a minimum and maximum amount of $-9.09 \, dB$ and $-17.51 \, dB$, respectively.

Finally, the optimization of both the static excitations and the on-off commutation instants is carried out. For comparative purposes, the same example dealt with in [9] has been considered. Fig. 7 shows the static amplitude coefficients [Fig. 7(a)] and the normalized pulse durations [Fig. 7(b)] obtained by means of the PSO-based approach. The pattern at the central frequency (Fig. 8) is characterized by $SLL^{opt} = -47 \, dB$ and $D^{max} = 24.3 \, dB$. Moreover, $\mathcal{P}_{SBR} \left(\underline{I}^{opt}, \underline{\tau}^{opt} \right) = 5.6\%$. After the optimization of the vector $\underline{t}^{on}$, where $H = 2$ has been set, the final values of SBL_h, for $h \in [1, 20]$ are given in Fig. 9. It is worth noting that the SBL has been lowered of more than $10 \, dB$ (form $-29.0 \, dB$ to $-40.1 \, dB$) and $11 \, dB$ (form $-29.6 \, dB$ to $-42.1 \, dB$) for $h = 1$ and $h = 2$, respectively.

4   Conclusions

In this paper, a strategy for the control of the sideband radiation in time-modulated planar array is presented and validated. By exploiting a closed-form expression of the power losses, the SBR has been minimized while synthesizing a desired pattern at the carrier frequency with a low peak sidelobe level. Moreover, the additional control of the on-off commutation instants has been used to reduce the SBL and to avoid high power levels within the main lobe region. A set of results from the two-stage PSO-based optimization approach has been shown to illustrate the effectiveness of the proposed approach.

References

[1] H. E. Shanks and R. W. Bickmore, "Four-dimensional electromagnetic radiators," *Canad. J. Phys.*, vol. 37, pp. 263-275, 1959.

[2] W. H. Kummer, A. T. Villeneuve, T. S. Fong , and F. G. Terrio, "Ultra-low sidelobes from time-modulated arrays," *IEEE Trans. Antennas Propag.,* vol. 11, no. 6, pp. 633-639, Nov. 1963.

[3] S. Yang, Z. Nie, and F. Yang, "Synthesis of low sidelobe planar antenna arrays with time modulation," in *Proc. APMC 2005 Asia-Pacific Microw. Conf.*, Suzhou, China, 4-7 Dec. 2005, vol. 3, pp. 3.

[4] Y. Chen, S. Yang, Z. Nie, "Synthesis of satellite footprint patterns from time-modulated planar arrays with very low dynamic range ratios," *Int. J. Numer. Model.*, vol. 21, pp. 493-506, 2008.

[5] J. Fondevila, J. C. Brégains, F. Ares, and E. Moreno, "Optimizing uniformly excited linear arrays through time modulation," *IEEE Antennas Wireless Propag. Lett.*, vol. 3, pp. 298-301, 2004.

[6] S. Yang, Y. B.Gan, A. Qing, and P. K. Tan, "Design of a uniform amplitude time modulated linear array with optimized time sequences," *IEEE Trans. Antennas Propag.,* vol. 53, no. 7, pp. 2337-2339, Jul. 2005.

[7] J. Fondevila, J. C. Brégains, F. Ares, and E. Moreno, "Application of time modulation in the synthesis of sum and difference patterns by using linear arrays," *Microw. Opt. Technol. Lett.,* vol. 48, no. 5, pp. 829-832, May 2006.

[8] S. Yang, Y. B. Gan, and A. Qing, "Sideband suppression in time-modulated linear arrays by the differential evolution algorithm," *IEEE Antennas Wireless Propag. Lett.,* vol. 1, pp. 173-175, 2002.

[9] S. Yang and Z. Nie, "Time modulated planar arrays with square lattices and circular boundaries," *Int. J. Numer. Model.*, vol. 18, pp. 469-480, 2005.

[10] Y. Chen, S. Yang, Z. Nie, "Synthesis of optimal sum and difference patterns from time-modulated hexagonal planar arrays," *Int. J. Infrared Milli. Waves*, vol. 29, pp. 933-945, 2008.

[11] C.A. Balanis, *Antenna Theory: Analysis and Design*. Hoboken, NJ: Wiley (3rd Ed.), 2005.

[12] M. I. Skolnik. *Radar Handbook.* New York, McGraw-Hill (3rd Ed.), 2008.

[13] J. C. Brégains, J. Fondevila, G. Franceschetti, and F. Ares, "Signal radiation and power losses of time-modulated arrays," *IEEE Trans. Antennas Propag.*, vol. 56, no. 6, pp. 1799-1804, Jun. 2008.

[14] L. Poli, P. Rocca, L. Manica, and A. Massa, "Handling sideband radiations in time-modulated arrays thorugh particle swarm optimization," *IEEE Trans. Antennas Propag.*, in press.

[15] P. Rocca and A. Massa, "Innovative approaches for optimized performance in time-modulated linear arrays," *Proc. 2009 IEEE Antennas & Propagation International Symp.*, Charleston, SC (USA), June 1-5, 2009, pp. 4.

[16] J. Kennedy, R. C. Eberhart, and Y. Shi, *Swarm Intelligence*. San Francisco, CA: Morgan Kaufmann, 2001.

[17] M. Donelli and A. Massa, "Computational approach based on a particle swarm optimizer for microwave imaging of two-dimensional dielectric scatterers," *IEEE Trans. Microw. Theory Tech.*, vol. 53, no. 5, pp. 1761-1776, May 2005.

[18] L. Manica, P. Rocca, L. Poli, and A. Massa, "Almost time-independent performance in time-modulated linear arrays ," *IEEE Antennas Wireless Propag. Lett.*, vol. 8, pp. 843-846, 2009.

[19] R. S. Elliott, *Antenna Theory and Design*. Hoboken, NJ: Wiley (2nd Ed.), 2003.

[20] P. Rocca, M. Benedetti, M. Donelli, D. Franceschini, and A. Massa, "Evolutionary optimization as applied to inverse problems," *Inverse Problems*, vol. 25, pp. 1-41, Dec. 2009.

FIGURE CAPTIONS

- **Figure 1.** Plot of (*a*) the Taylor quiescent pattern ($\tau_{mn} = 1$, $\forall mn$) and of (*b*) the corresponding static excitations $\underline{I} = \underline{I}^T$.

- **Figure 2.** Plot of (*a*) the distribution of $\underline{\tau}^{opt}$ and of (*b*) the corresponding pattern radiated at the carrier frequency ($h = 0$, $SLL = -37.8\,dB$).

- **Figure 3.** Normalized power patterns at (*a*) the first ($|h| = 1$, $SBL_1 = -16.15\,dB$) and (*b*) the second ($|h| = 2$, $SBL_2 = -21.88\,dB$) harmonic radiation when optimizing the functional Ψ_{SBR}.

- **Figure 4.** Element on-off time sequence when optimizing Ψ_{SBR} and Ψ_{SBL}.

- **Figure 5.** Normalized power patterns at (*a*) the first ($|h| = 1$, $SBL_1 = -33.66\,dB$) and (*b*) the second ($|h| = 2$, $SBL_1 = -32.10\,dB$) harmonic radiations when optimizing the functional Ψ_{SBL}.

- **Figure 6.** Behavior of the sideband levels, SBL_h, $h \in [0,\,20]$.

- **Figure 7.** Plot of the distribution of (a) $\underline{I}^{opt}$ and of (*b*) $\underline{\tau}^{opt}$.

- **Figure 8.** Normalized power pattern radiated at the carrier frequency ($h = 0$, $SLL = -47\,dB$).

- **Figure 9.** Behavior of the sideband levels, SBL_h, $h \in [0,\,20]$.
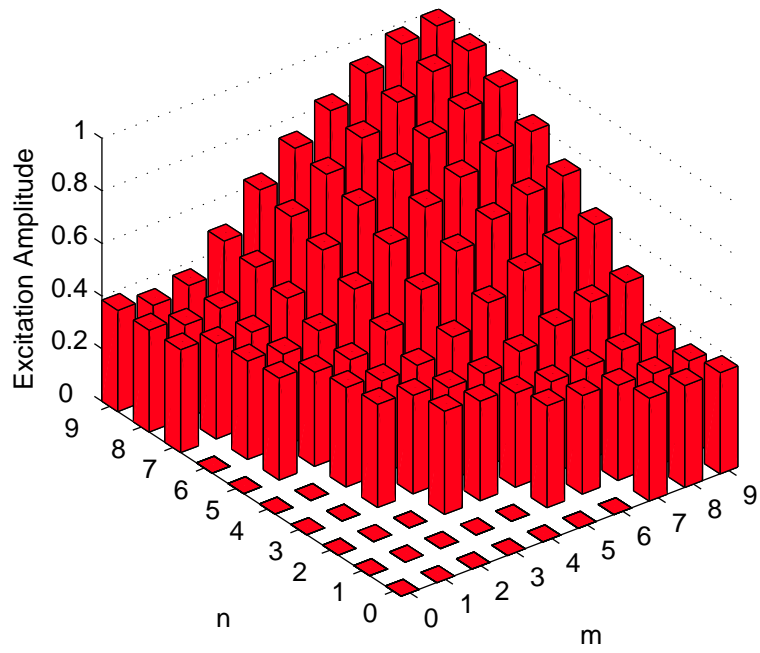
(a)
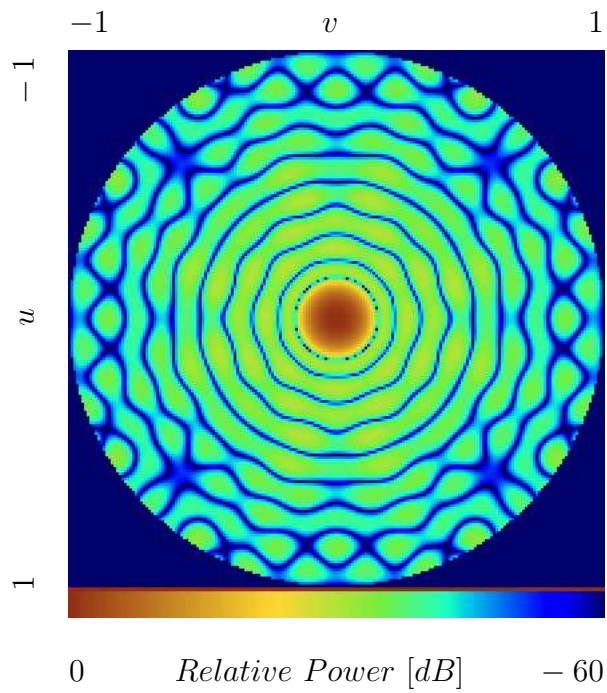
(b)

Fig. 1 - P. Rocca *et al.,* "Synthesis of Time-Modulated Planar Arrays ..."
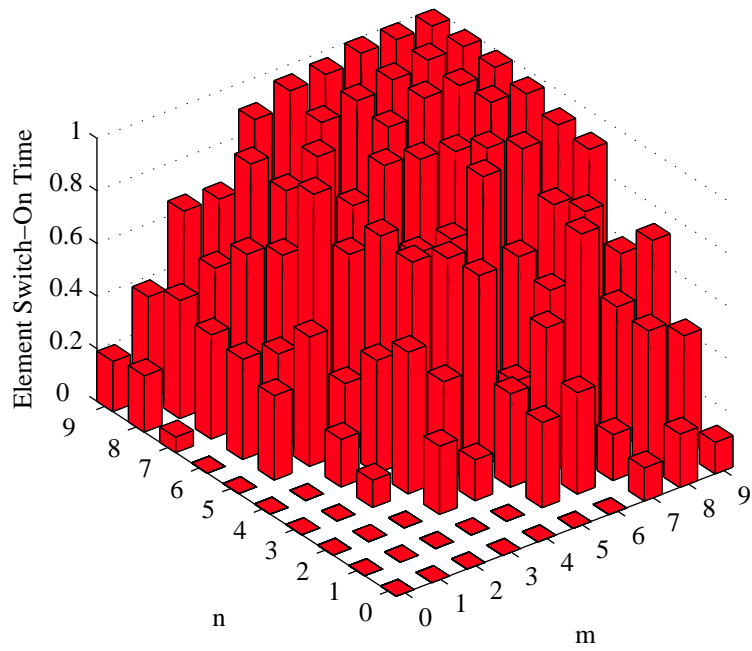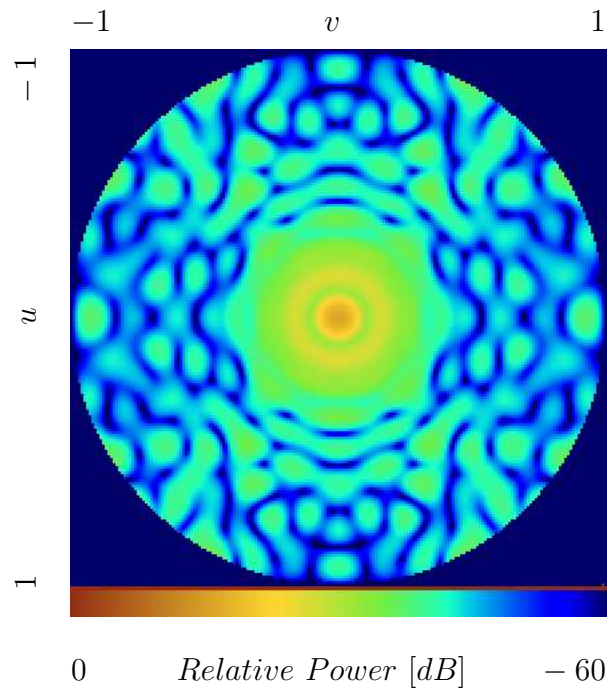
(a)
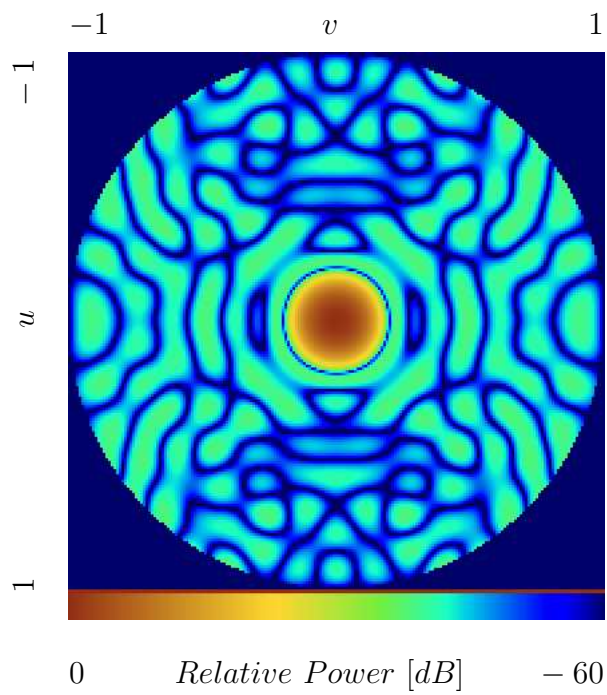
(b)

Fig. 2 - P. Rocca *et al.*, "Synthesis of Time-Modulated Planar Arrays ..."

13

(a)

(b)
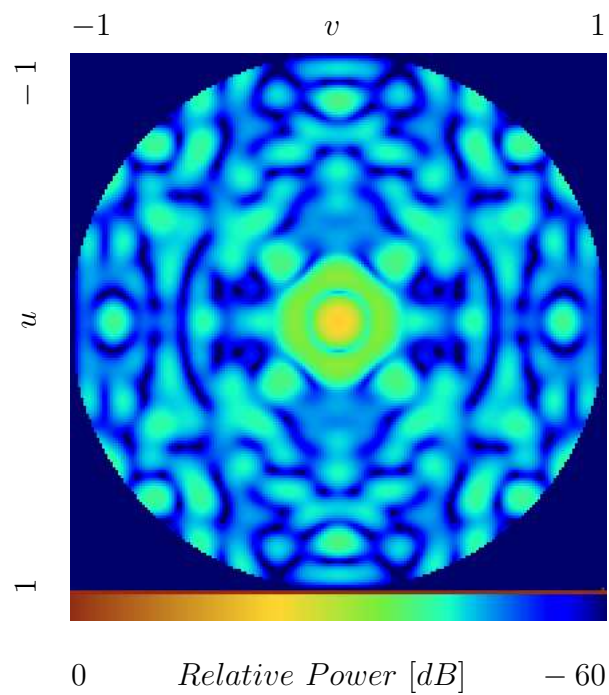
Fig. 3 - P. Rocca *et al.,* "Synthesis of Time-Modulated Planar Arrays ..."

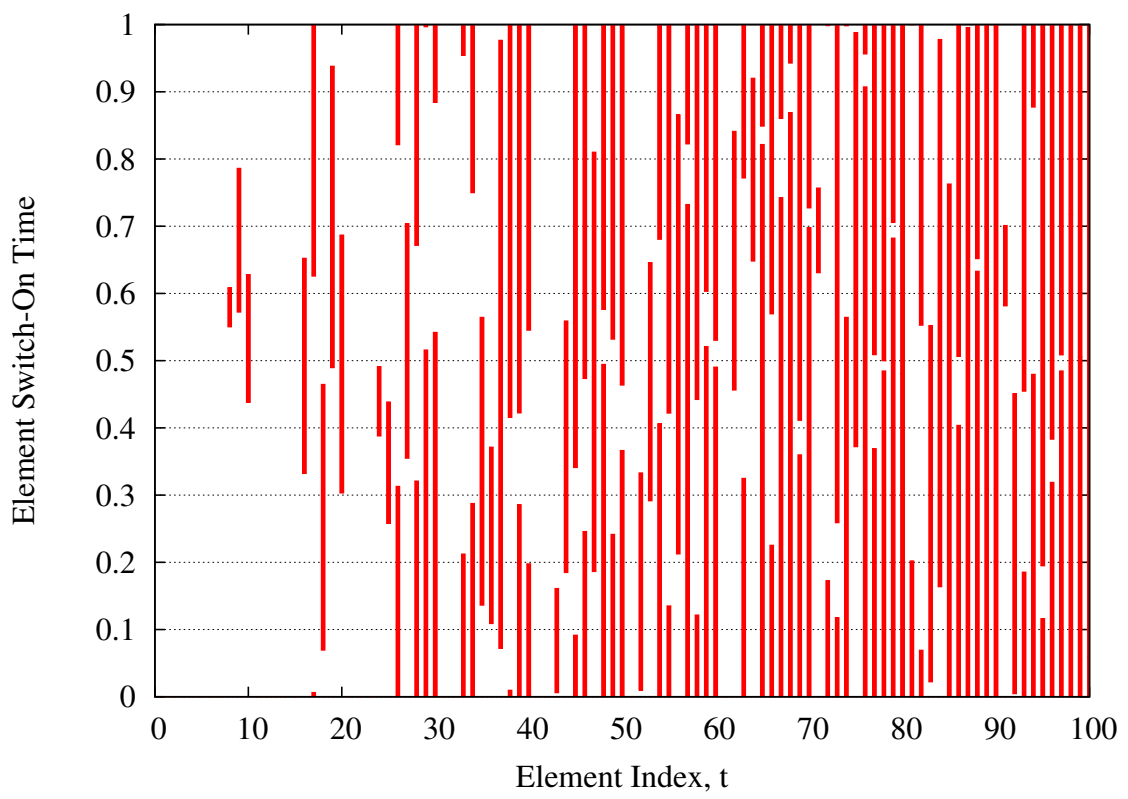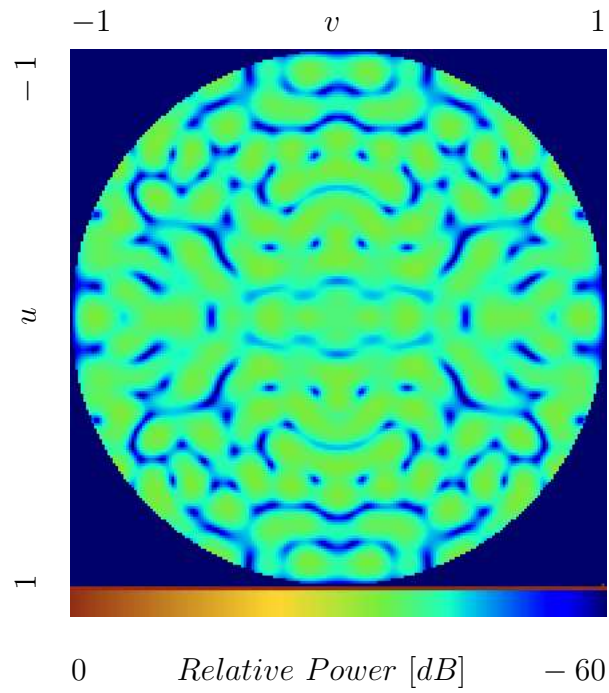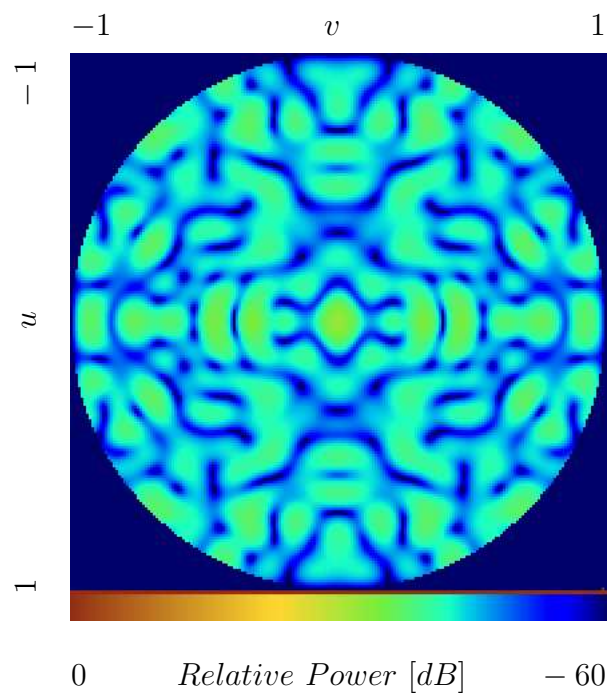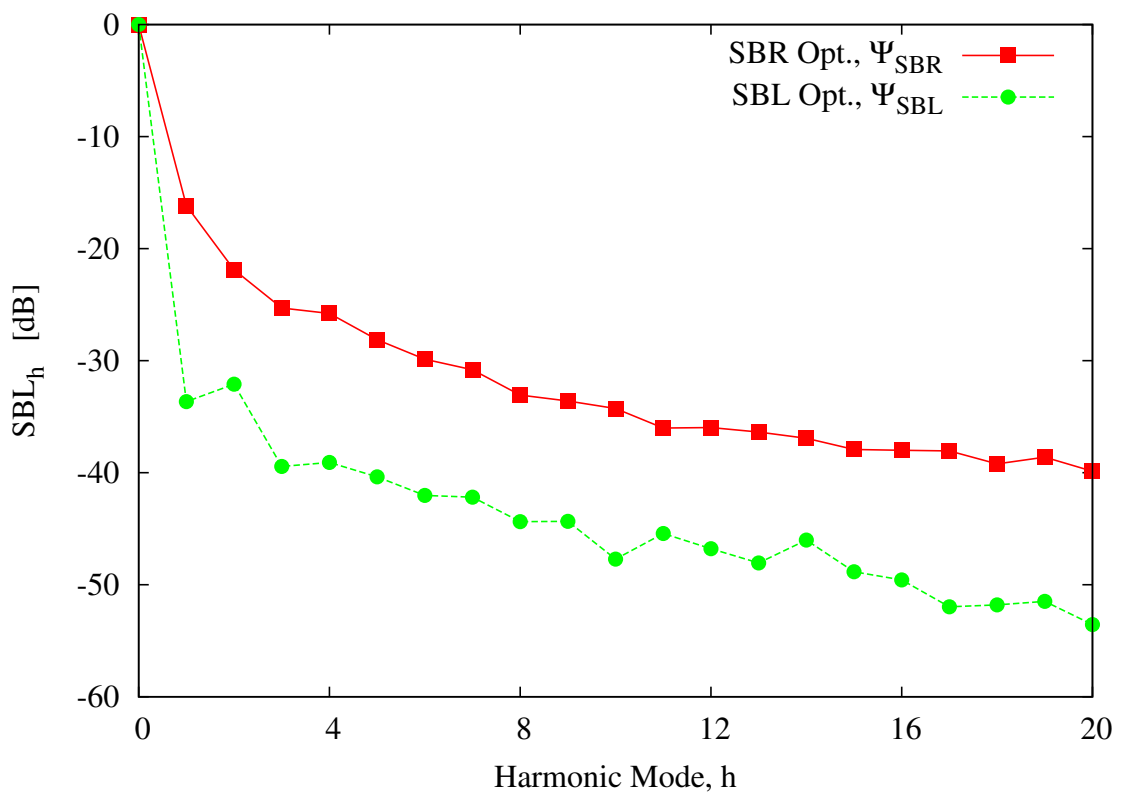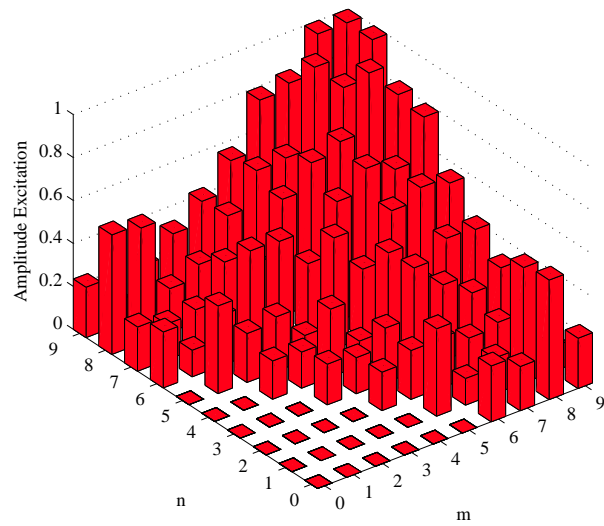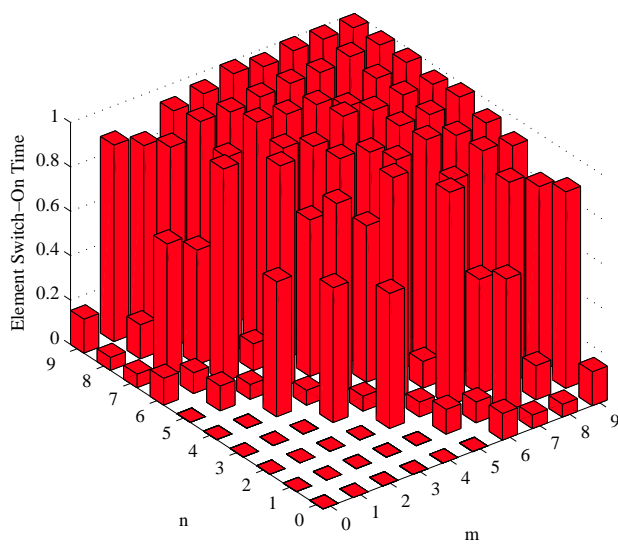**Fig. 4 - P. Rocca *et al.,*** "Synthesis of Time-Modulated Planar Arrays ..."

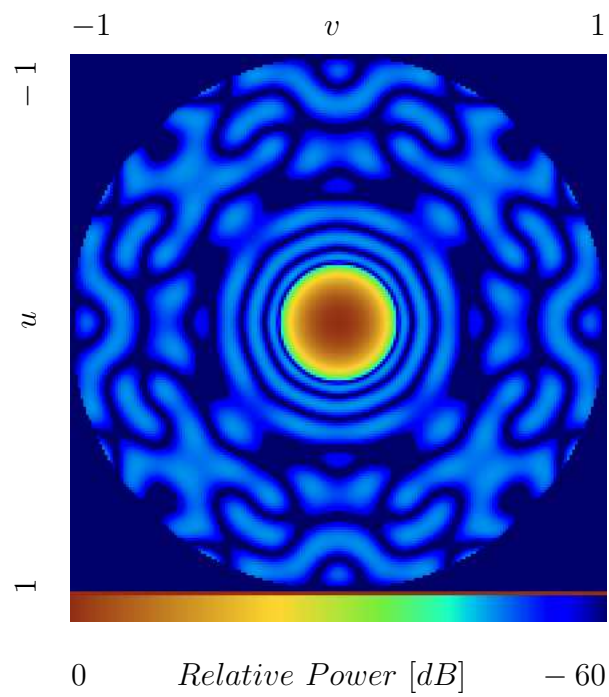15

(a)

(b)

Fig. 5 - P. Rocca *et al.,* "Synthesis of Time-Modulated Planar Arrays ..."

Fig. 6 - P. Rocca *et al.,* "Synthesis of Time-Modulated Planar Arrays ..."
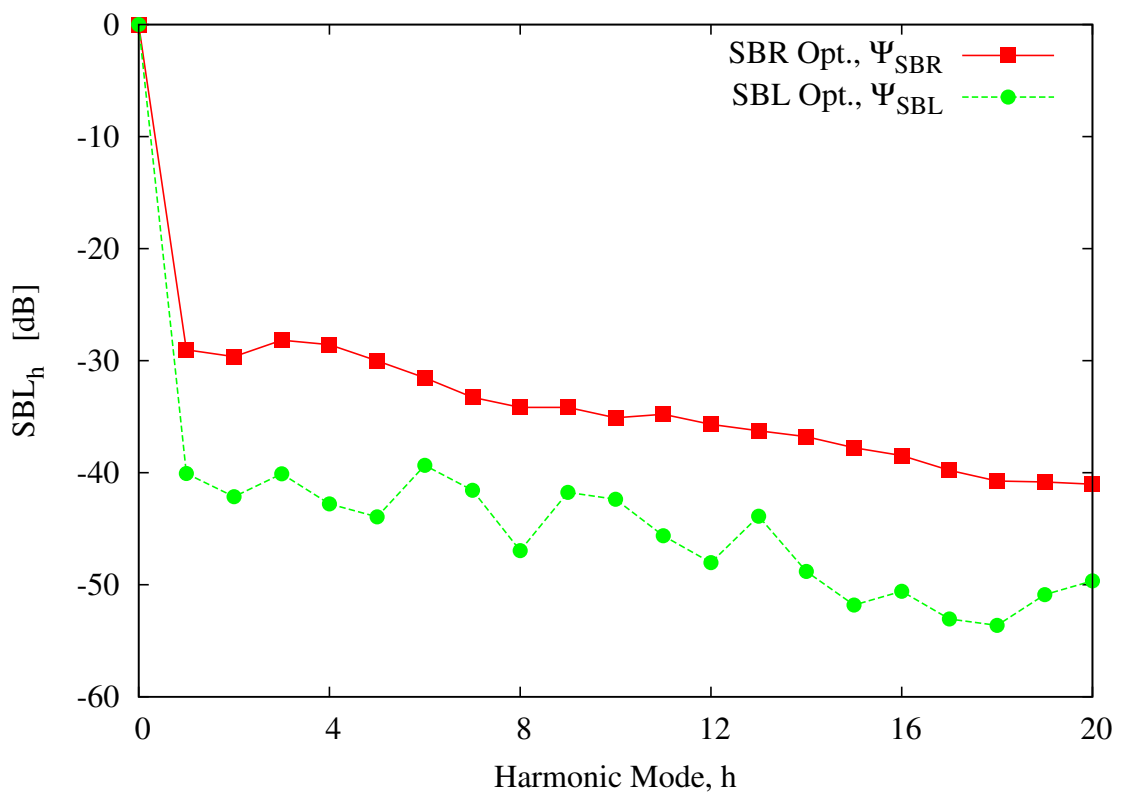
(*a*)

(*b*)

Fig. 7 - P. Rocca *et al.*, "Synthesis of Time-Modulated Planar Arrays ..."

18

Fig. 8 - P. Rocca *et al.,* "Synthesis of Time-Modulated Planar Arrays ..."

Fig. 9 - P. Rocca *et al.,* "Synthesis of Time-Modulated Planar Arrays ..."